

UC Berkeley

UC Berkeley Previously Published Works

Title

Neoproterozoic to early Phanerozoic rise in island arc redox state due to deep ocean oxygenation and increased marine sulfate levels

Permalink

<https://escholarship.org/uc/item/3cf1s72v>

Journal

Proceedings of the National Academy of Sciences of the United States of America, 116(18)

ISSN

0027-8424

Authors

Stolper, Daniel A
Bucholz, Claire E

Publication Date

2019-04-30

DOI

10.1073/pnas.1821847116

Peer reviewed

Neoproterozoic to early Phanerozoic rise in island arc redox state due to deep ocean oxygenation and increased marine sulfate levels

Daniel A. Stolper^{a,b,1} and Claire E. Bucholz^{c,1}

^a Department of Earth and Planetary Science, University of California, Berkeley, CA 94720; ^b Earth and Environmental Sciences Area, Lawrence Berkeley National Laboratory, Berkeley, CA 94720; and ^c Division of Geological and Planetary Sciences, California Institute of Technology, Pasadena, CA 91125

Significance

Igneous island arc rocks are more oxidized than midocean-ridge basalts. Whether this originates from an oxidized mantle source or during differentiation or eruption is debated. Newly compiled $\text{Fe}^{3+}/\Sigma\text{Fe}$ and V/Sc ratios presented here indicate that island arc rocks became more oxidized 800–400 Ma. We attribute this increase in the redox state of island arc rocks to the oxidation of their mantle source from subduction of oxidized oceanic crust following deep-ocean oxygenation and increased marine sulfate concentrations over the same time interval. This provides evidence that the oxidized nature of modern island arc magmas is due to an oxidized mantle source and represents a rare example of a change in the surface biogeochemistry influencing the igneous rock record.

Abstract

A rise in atmospheric O_2 levels between 800 and 400 Ma is thought to have oxygenated the deep oceans, ushered in modern biogeochemical cycles, and led to the diversification of animals. Over the same time interval, marine sulfate concentrations are also thought to have increased to near-modern levels. We present compiled data that indicate Phanerozoic island arc igneous rocks are more oxidized ($\text{Fe}^{3+}/\Sigma\text{Fe}$ ratios are elevated by 0.12) vs. Precambrian equivalents. We propose this elevation is due to increases in deep-ocean O_2 and marine sulfate concentrations between 800 and 400 Ma, which oxidized oceanic crust on the seafloor. Once subducted, this material oxidized the subarc mantle, increasing the redox state of island arc parental melts, and thus igneous island arc rocks. We test this using independently compiled V/Sc ratios, which are also an igneous oxybarometer. Average V/Sc ratios of Phanerozoic island arc rocks are elevated (by +1.1) compared with Precambrian equivalents, consistent with our proposal for an increase in the redox state of the subarc mantle between 800 and 400 Ma based on $\text{Fe}^{3+}/\Sigma\text{Fe}$ ratios. This work provides evidence that the more oxidized nature of island arc vs. midocean-ridge basalts is related to the subduction of material oxidized at the Earth's surface to the subarc mantle. It also indicates that the rise of atmospheric O_2 and marine sulfate to near-modern levels by the late Paleozoic influenced not only surface biogeochemical cycles and animal

diversification but also influenced the redox state of island arc rocks, which are building blocks of continental crust.

Main

Sometime between 800 and 400 Ma, atmospheric O₂ concentrations are thought to have risen to sufficient concentrations (~10 to 50% of modern levels) to oxygenate the majority of the deep oceans (e.g., refs. 1–10). This transition has been of long-standing interest as it marks a fundamental shift in the biogeochemical cycles on Earth's surface to those similar to what is seen today and has been linked to the proliferation of animals (e.g., refs. 1, 2, 5, 6, 11, and 12). Additionally, over this same time interval marine sulfate concentrations are thought to have increased by as much as ~10-fold and reached near-modern levels (e.g., refs. 13–17). Increases in marine sulfate and deep-ocean O₂ concentrations at this time have been proposed to have led to an increase in the redox state of oceanic crust via oxidation during hydrothermal circulation of oxygenated water (10) and/or circulation of seawater-derived sulfate (18, 19) through this crust. Before the oxygenation of the deep ocean and the rise in seawater sulfate levels these oxidative processes are likely to have been significantly diminished.

Igneous rocks from modern arc environments are well known to be oxidized relative to midocean-ridge basalts (MORB) (e.g., refs. 20–24). Understanding the origin of this difference has been of enduring interest as the elevated redox state, often reported in terms of oxygen fugacity (fO_2), of arc basalts relative to MORB has been proposed to control their differing mineral assemblages and thus differing trends in chemical composition (e.g., ref. 20), as well as the formation of arc-associated economic gold and copper deposits (e.g., ref. 25). One leading hypothesis for the origin of the elevated fO_2 values of arc rocks vs. MORB is that oxidized material derived from subducting slabs oxidizes the mantle source of arc magmas (i.e., the subarc mantle) (18, 21, 24, 26–30). Based on this, it has been hypothesized that an increase in the redox state of subducting slabs due to the oxygenation of the deep ocean and increased marine sulfate concentrations could be reflected by an elevation in the fO_2 of igneous arc rocks in the Phanerozoic relative to in the Precambrian (10, 18, 19). However, whether the fO_2 of arc rocks has or has not changed with time is neither known nor has it been directly evaluated.

Note that from this point on we use “redox state” to describe the relative balance of oxidized vs. reduced elements (e.g., Fe³⁺ vs. Fe²⁺ or S⁶⁺ vs. S²⁻) in any rock, including both pristine igneous rocks and those that may have experienced secondary (i.e., subsolidus) alteration (e.g., oxidation by oxygenated waters). We use oxygen fugacity (fO_2), which is the fugacity of O₂ in a magma or rock assemblage at a specified temperature and pressure, only for the description of the redox state of what are considered primary (i.e., unaltered) igneous mineral assemblages and melts. Finally, when fO_2 values of differing rock types (e.g., island arc rocks vs. MORB) are

compared this is always done implicitly relative to an igneous redox buffer [e.g., quartz–fayalite–magnetite (QFM)].

To test this hypothesis, we compiled two geochemical parameters for island arc rocks through time that have been widely used to estimate the fO_2 of igneous rocks and their mantle sources, specifically $Fe^{3+}/\Sigma Fe$ (i.e., molar $Fe^{3+}/[Fe^{2+}+Fe^{3+}]$) (e.g., refs. 24 and 31) and V/Sc ratios (32–35). Both ratios positively covary with source rock fO_2 . V/Sc ratios were chosen over other proposed trace-element-ratio oxybarometers such as Zn/Fe (36), V/Ga (34), and V/Yb (37) as V/Sc is the only one that has been widely applied to quantitatively reconstruct the fO_2 of modern basalts (including island arcs and MORB) and ancient (i.e., Precambrian) igneous rocks (32–35, 38). Island arc rocks were chosen for this study over continental arc rocks as their parental magmas neither transit through nor crystallize in older continental crust, which, if assimilated, could change their redox state.

Our proposed test is simple: (i) If the oxygenation of the deep ocean and concomitant increase in marine sulfate concentration caused a significant increase in the redox state of oceanic crustal material subducted into the mantle and (ii) this oxidized material influences the fO_2 of the mantle source of island arc magmas, then it follows that both $Fe^{3+}/\Sigma Fe$ and V/Sc ratios of igneous rocks from island arc environments should increase around the time of the Neoproterozoic–Phanerozoic boundary (~540 Ma).

This test may fail for a variety of reasons. First, $Fe^{3+}/\Sigma Fe$ ratios are susceptible to modification during melt differentiation, degassing, metamorphism, and exposure to the atmosphere, and such processes could obscure any primary information on the redox state of the source of island arcs. Second, serpentinization of ultramafic rocks also leads to the oxidation of oceanic crust and the upper lithosphere that is transported to the mantle during subduction and, therefore, could also lead to the oxidation of the subarc mantle (e.g., ref. 39). Although the degree of serpentinization of oceanic lithosphere is uncertain (one order of magnitude uncertainty; ref. 40), this process could have led to a sufficient flux of subducted oxidized material to oxidize island arc mantle sources since the initiation of subduction. Importantly, this would allow for the oxidation of the subarc mantle without invoking the involvement of oceanic crust oxidized by marine dissolved O_2 or sulfate. Third, it has been proposed that the fO_2 of the mantle sources of island arc rocks and MORB are similar (33, 34, 36, 41) or even that some primary arc melts can be more reduced than MORB (42). If this is correct, then the processes that cause the elevated redox state of island arc volcanic rocks must occur instead during ascent, melt differentiation, and/or eruption (33, 34, 36, 41, 43). If island arc rocks are more oxidized vs. MORB due to the subduction of oxidized serpentinite or due to melt differentiation or eruption, then no temporal change in the $Fe^{3+}/\Sigma Fe$ or V/Sc ratios of island arc rocks would be predicted—for example, being uniformly elevated in island arc igneous rocks relative to MORB at all ages in the first case or

uniform and similar in primitive, undegassed island arc igneous rocks (or even reduced) relative to primitive MORB at all ages in the second case.

Materials and Methods

We compiled $\text{Fe}^{3+}/\Sigma\text{Fe}$ and V/Sc ratios of both extrusive and intrusive rocks previously interpreted to have formed in island arc environments from 3.1 billion years ago to the present. Implicitly, we have made the common assumption that plate tectonics and thus subduction began in the Archean, although the timing continues to be debated (see discussion in refs. 44 and 45). Island arc localities were identified based on trace-element arguments (e.g., refs. 46–48), field relationships and lithologic associations (e.g., volcanoclastic sedimentary rocks and paired metamorphic belts), presence of boninites (e.g., refs. 49 and 50), geochronology supporting a tectonic history as an island arc, and prior compilations (e.g., refs. 51 and 52)—all localities have previously and independently interpreted as ancient island arcs. Details of each locality are given in Dataset S1, including which of the above criteria were fulfilled for each locality. In general, most localities had at least two of the above criteria met; however, identification of Paleoproterozoic and Archean localities was primarily based on trace element arguments. We note that Dataset S1 is not meant to represent a comprehensive list of all island arc localities in the geologic record, but rather those for which whole-rock $\text{Fe}^{3+}/\Sigma\text{Fe}$ and/or V/Sc ratios were available.

Insofar as it was possible, cumulates were avoided for both records. Metamorphic grade for the localities, when reported, varied from unmetamorphosed to amphibolite facies and did not vary systematically with age (Dataset S1). $\text{Fe}^{3+}/\Sigma\text{Fe}$ values are based on whole-rock wet chemical extractions (all data in Dataset S2 and locality averages in Dataset S3). For $\text{Fe}^{3+}/\Sigma\text{Fe}$ ratios, subaerially erupted rocks were excluded (again insofar as it was possible) to avoid samples potentially oxidized by atmospheric O_2 during eruption following the initial oxygenation of the atmosphere ~2.4 to 2.3 billion years ago (e.g., refs. 5 and 11).

For the V/Sc compilation (all data in Dataset S4 and locality averages in Dataset S5), rocks were avoided that showed obvious evidence of clinopyroxene crystallization, which modifies V/Sc ratios (e.g., refs. 32 and 53). Following previous workers (32–35, 53), we used a MgO weight percent cutoff to select samples derived from melts that did not undergo clinopyroxene crystallization. We chose a value of 6.5 wt % MgO (with samples needing to have >6.5 wt % MgO) based on an examination of where CaO begins to decrease when CaO vs. MgO is plotted for precompiled island arc igneous rocks from the GEOROC database (georoc.mpch-mainz.gwdg.de/georoc/Entry.html). This break in slope marks the onset of clinopyroxene crystallization and typically occurs in this database between 5 and 6.5 wt % MgO. Our MgO cutoff is lower than that used previously for MORB (8 wt % MgO; ref. 32) as the presence of water in island arc parental

melts expands the stability field of olivine relative to pyroxene (e.g., ref. 54) but is consistent with previous MgO cutoffs used in studies of V and Sc in island arc rocks (5 to 6 wt %; refs. 34 and 53). We also excluded rocks with >15 wt % MgO to avoid incorporation of samples derived from exceptionally high degrees of melt or that represent a mixture of melt and accumulated olivine (e.g., ref. 32). As discussed below, the precise choice of the MgO cutoff does not affect any of our interpretations. We also present previously compiled MORB V/Sc ratios from Gale et al. (55) for comparison as well as compilations of V/Sc for ancient basalts used previously to reconstruct the fO_2 of the upper mantle (32, 35). For these, as was the case for our treatment of MORB, we again selected samples with MgO contents between 8 and 15 wt %.

Results and Discussion

Fe³⁺/ΣFe Ratios of Island Arc Igneous Rocks Through Time.

Fe³⁺/ΣFe ratios of igneous rocks and melt inclusions have been used extensively to reconstruct the fO_2 of the parental melts of young igneous rocks, for example MORB dredged from the seafloor or samples taken from active island arcs (e.g., refs. 31, 22, 56, 24, and 57–60). We use this approach on whole rocks to attempt to reconstruct the redox state of island arc rocks through time. Glasses are preferred for Fe³⁺/ΣFe-based fO_2 reconstructions as they are quenched melts. In using whole rocks, we follow previous workers in assuming that examined whole rocks are representative of the bulk composition of the melt from which they crystallized (e.g., refs. 56 and 60).

Use of whole-rock Fe³⁺/ΣFe ratios from ancient (i.e., Precambrian) samples for the purpose of reconstructing the original redox state of a sample is uncommon due to the typical assumption that Fe³⁺/ΣFe ratios of ancient samples may be compromised by metamorphism or hydrothermal alteration (e.g., ref. 61). As such, it is critical to evaluate the possible effects of alteration and metamorphism on the compiled whole-rock Fe³⁺/ΣFe ratios, which we do below. We first present the compiled Fe³⁺/ΣFe ratios to see if there are any differences in Fe³⁺/ΣFe ratios of igneous island arc rocks as a function of time. Then we evaluate, through a variety of tests, whether the Fe³⁺/ΣFe ratios are controlled by primary or secondary processes (e.g., oxidation by atmospheric O₂ before collection in the field, metamorphic/hydrothermal alteration, degassing, or differentiation). Following this, we use a completely different oxybarometer, V/Sc, to independently test our interpretations.

Fig. 1 shows the average Fe³⁺/ΣFe ratios for each island arc locality vs. age. An increase in Fe³⁺/ΣFe ratios around the Precambrian–Cambrian boundary (541 Ma) is visually apparent. Data histograms are given in *SI Appendix*, Fig. S1. To test whether there is a significant difference in average Fe³⁺/ΣFe ratios of igneous island arc rocks from the Phanerozoic vs. the Precambrian, we calculated the average Fe³⁺/ΣFe ratios over a given age range based on the

average $\text{Fe}^{3+}/\Sigma\text{Fe}$ ratio of each locality in that age range. For this test, we chose the following age ranges: the Late Paleozoic to Cenozoic (420 to 0 Ma), the Early Paleozoic (541 to 420 Ma), and the Precambrian (>541 Ma). These age ranges allow us to explicitly test the hypothesis posed above as to whether island arc rocks are more oxidized in the Phanerozoic vs. the Precambrian following the oxygenation of the deep ocean and increased marine sulfate concentrations ~800 to 400 Ma. The Early Paleozoic is separated as its own group because some recent studies indicate the large-scale oxygenation of the deep ocean occurred during or after this time interval (2, 6, 9, 10). The Neoproterozoic (1,000 to 541 Ma), which has also been proposed to be a time of increasing atmospheric O_2 (e.g., refs. 1, 3, 5, 7, and 12), is not treated separately here due to the limited number of arc localities available from this time frame ($n = 5$). However, treating the Neoproterozoic as a separate group for $\text{Fe}^{3+}/\Sigma\text{Fe}$ ratios does not change our conclusions.

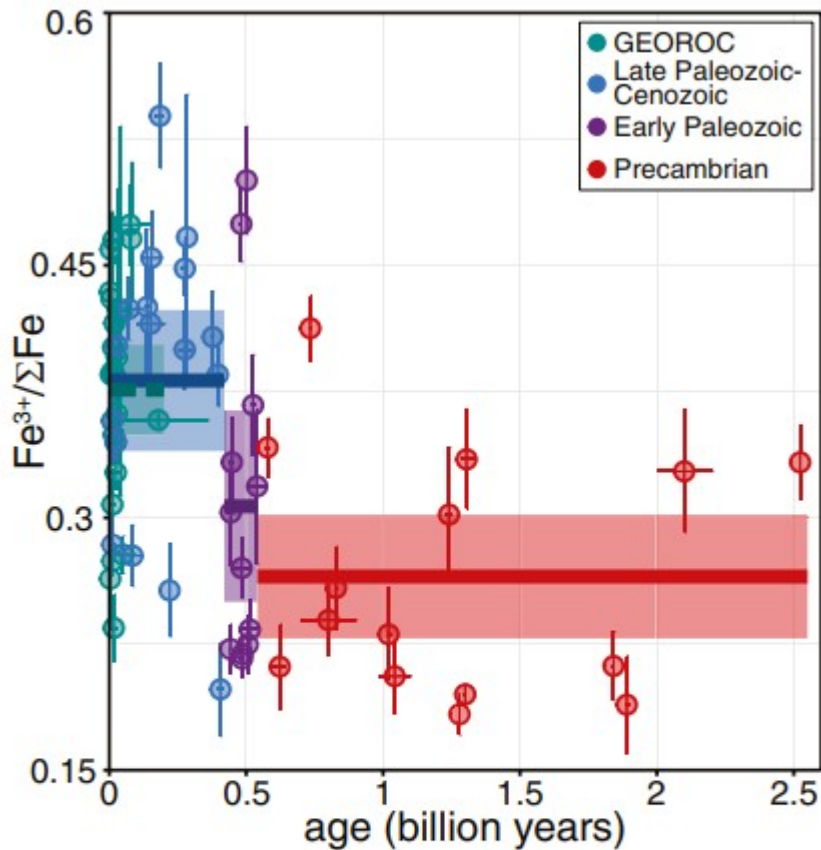


Fig. 1. Average $\text{Fe}^{3+}/\Sigma\text{Fe}$ ratios of island arcs rocks through time. Each data point is the average value of a specific island arc locality. Data include both intrusive and extrusive igneous rocks. Solid horizontal lines are averages of the locality means over the given time period: 0.265 ± 0.018 (1 SE) for the Precambrian, 0.307 ± 0.028 for the Early Paleozoic, and 0.382 ± 0.021 for Late Paleozoic–Cenozoic. Shading represents 2 SE. Vertical error bars for individual points are 1 SE. Horizontal age uncertainties vary depending on the age constraints available for each island arc (Dataset S1).

Mean $\text{Fe}^{3+}/\Sigma\text{Fe}$ ratios for the chosen age ranges are 0.265 ± 0.018 (1 SE; 15 localities, 367 analyses) for the Precambrian, 0.307 ± 0.028 (12 localities, 317 analyses) for the Early Paleozoic, and 0.382 ± 0.021 (17 localities, 528 analyses) for Late Paleozoic–Cenozoic (<420 Ma) (Fig. 1). Our average $\text{Fe}^{3+}/\Sigma\text{Fe}$ ratio for Late Paleozoic–Cenozoic island arc rocks are similar to mean values of similarly aged island arcs based on data from precompiled igneous island arc rocks from GEOROC, 0.376 ± 0.013 (1 SE) (Fig. 1), and a value of 0.38 as given by Lécuyer and Ricard (23). The mean value for the Late Paleozoic–Cenozoic is significantly different ($P < 0.05$) from the Precambrian mean value ($P = 0.0005$; Tukey’s honestly significant difference test), while the Early Paleozoic mean is neither statistically distinct ($P > 0.05$) from the Late Paleozoic–Cenozoic mean ($P = 0.07$) nor the Precambrian mean ($P = 0.52$). This indicates that mean $\text{Fe}^{3+}/\Sigma\text{Fe}$ ratios of igneous island arc rocks from Phanerozoic are indeed statistically more elevated than those

from the Precambrian. Finally, we examined the fidelity of our choice of age bins by fitting a moving average to the data (*SI Appendix*, Fig. S2). This approach also shows an increase in $\text{Fe}^{3+}/\Sigma\text{Fe}$ after 541 Ma and is thus consistent with our analysis above.

The average Late Paleozoic–Cenozoic island arc rock $\text{Fe}^{3+}/\Sigma\text{Fe}$ ratio of ~ 0.38 is elevated compared with typical measurements of $\text{Fe}^{3+}/\Sigma\text{Fe}$ based on Fe K-edge X-ray absorption near-edge structure (XANES) measurements of modern island arc glasses from, for example, the Marianas [0.239 ± 0.003 (1 SE) (58, 59, 62)] and Vanuatu [0.283 ± 0.019 (63)]. To better understand this difference, we compared measurements of $\text{Fe}^{3+}/\Sigma\text{Fe}$ ratios based on wet chemical extractions from GEOROC vs. XANES measurements on igneous rocks from these two island arc localities as well as Hawaii (*SI Appendix*, Fig. S3 and ref. 64). Whole-rock $\text{Fe}^{3+}/\Sigma\text{Fe}$ ratios from GEOROC are offset to higher values compared with XANES-based estimates of glasses by, on average, 0.074 ± 0.024 (1σ). The distributions also differ in that the whole-rock samples show a tail to elevated $\text{Fe}^{3+}/\Sigma\text{Fe}$ that is not present in the XANES data (*SI Appendix*, Figs. S1 and S3). When distributions are unimodal (e.g., for Marianas and Hawaii) the modes of the smoothed distributions of the whole-rock and XANES data are similar (within 0.015; *SI Appendix*, Fig. S3). A similar difference is also observed when comparing $\text{Fe}^{3+}/\Sigma\text{Fe}$ values of ancient submarine basalts preserved on the continents (i.e., ophiolites) vs. XANES on MORB. That is, average $\text{Fe}^{3+}/\Sigma\text{Fe}$ ratios for Precambrian submarine basalts from ophiolites range from 0.20 to 0.26 (10), 0.06 to 0.12 higher than that determined by XANES for modern MORB (0.14; ref. 65). Precambrian whole-rock samples were used for this comparison to avoid issues associated with oxidative alteration of MORB during hydrothermal circulation that is hypothesized to have occurred in Phanerozoic samples (10).

We interpret the elevated $\text{Fe}^{3+}/\Sigma\text{Fe}$ ratios of the whole-rock vs. XANES data (*SI Appendix*, Figs. S1 and S3) as being due to a small amount of oxidation of samples on Earth's surface. This oxidation appears to bias average whole-rock $\text{Fe}^{3+}/\Sigma\text{Fe}$ ratios to slightly above (~ 0.074) eruptive values but is not an issue for XANES measurements as these are made on pristine, unaltered glasses. As our compilation is based on submarine rocks, oxidation by atmospheric O_2 during eruption is not the cause of elevated whole-rock vs. XANES $\text{Fe}^{3+}/\Sigma\text{Fe}$ ratios. The GEOROC data include samples from both subaerial and submarine settings. It has a mean $\text{Fe}^{3+}/\Sigma\text{Fe}$ ratio similar (within 0.01) to our compilation of submarine rocks. This likely indicates that oxidative alteration by atmospheric O_2 during eruption does not strongly bias the GEOROC data for subaerially erupted samples. Rather, we propose that the elevated whole-rock vs. XANES $\text{Fe}^{3+}/\Sigma\text{Fe}$ ratios are most plausibly due to recent subaerial exposure on the Earth's surface following crystallization and exposure as otherwise the Precambrian submarine basalts would not also show this elevation. This is because these older samples formed in environments (the deep ocean) that are thought to have been essentially devoid of O_2 (e.g., refs. 5 and 11). We expect that any oxidation that has

occurred recently during exposure would affect the mean $\text{Fe}^{3+}/\Sigma\text{Fe}$ ratios of all of the localities approximately equally regardless of age as we are unaware of any reason that ancient samples exposed at Earth's surface would oxidize significantly more slowly in the presence of modern atmospheric O_2 than younger samples. We discuss the effects of oxidation by dissolved O_2 due to temporal changes in marine dissolved O_2 concentrations in the next section.

Finally, we tested whether the presence of a small number of highly oxidized samples (presumably via oxidation by modern atmospheric O_2) biases our record such that more highly oxidized and altered samples are Phanerozoic in age. To conduct this test, we filtered our dataset such that samples with $\text{Fe}^{3+}/\Sigma\text{Fe}$ ratios >0.8 , 0.7 , 0.6 , or 0.5 were excluded (*SI Appendix*, Table S1). Differences in mean $\text{Fe}^{3+}/\Sigma\text{Fe}$ ratios between the Precambrian vs. Late Paleozoic samples change from a maximum difference of $0.116 (\pm 0.028, 1 \text{ SE})$ without any filter to a minimum difference of $0.089 (\pm 0.022, 1 \text{ SE})$ with removal of all samples with $\text{Fe}^{3+}/\Sigma\text{Fe} > 0.5$. This shows that the differences we observe between Precambrian and Late Paleozoic–Cenozoic samples are not driven by a small number of samples with exceptionally high $\text{Fe}^{3+}/\Sigma\text{Fe}$ ratios.

Based on these tests, we proceed based on the working hypothesis that the averages of the compiled $\text{Fe}^{3+}/\Sigma\text{Fe}$ ratios in each age range can be used to understand relative changes in $\text{Fe}^{3+}/\Sigma\text{Fe}$ values with time. However, the observed systematic (though small) elevation in whole-rock $\text{Fe}^{3+}/\Sigma\text{Fe}$ ratios relative to XANES measurements, (which we interpreted above to indicate that whole-rock samples are commonly slightly oxidized postcrystallization) makes it challenging to use the $\text{Fe}^{3+}/\Sigma\text{Fe}$ values to calculate the $f\text{O}_2$ of the magmas accurately; therefore, we do not attempt this here.

Causes of the Elevated Phanerozoic vs. Precambrian $\text{Fe}^{3+}/\Sigma\text{Fe}$ Ratios of Island Arc Rocks.

We now explore several possible explanations for the origin of the increase in the average island arc rock $\text{Fe}^{3+}/\Sigma\text{Fe}$ values from ~ 0.27 to 0.38 from the Precambrian to the late Paleozoic. This increase with time could result from a variety of secular changes, including (i) temporal changes in the nature or degree of alteration or metamorphism, (ii) changes in the degree of differentiation or degassing of island arc magmas with time, or (iii) changes in the $f\text{O}_2$ of island arc mantle sources with time.

Temporal changes in the nature or degree of alteration or metamorphism.

One possibility is that the observed changes in $\text{Fe}^{3+}/\Sigma\text{Fe}$ ratios with time could result from postdepositional alteration of island arc igneous rocks caused either by a general reductive metamorphism of ancient samples (with Precambrian samples originally being more oxidized) relative to younger samples or to increased seafloor oxidation of younger arc samples (with Phanerozoic samples being originally more reduced than their current

levels). As iron is the main redox active element in igneous rocks, closed-system metamorphism will only redistribute Fe^{3+} and Fe^{2+} among different mineral assemblages but will not change whole-rock $\text{Fe}^{3+}/\Sigma\text{Fe}$ ratios (66). In contrast, open-system metamorphism can introduce reductants or oxidants to the system and thus can alter whole-rock $\text{Fe}^{3+}/\Sigma\text{Fe}$ ratios (66).

The lower $\text{Fe}^{3+}/\Sigma\text{Fe}$ ratios for Precambrian vs. Late Paleozoic and younger rocks could be unrelated to original rock redox states if metamorphism is typically reducing given that older rocks have a greater likelihood to be metamorphosed than younger rocks. Stolper and Keller (10) presented arguments for why metamorphism does not appear to universally lower $\text{Fe}^{3+}/\Sigma\text{Fe}$ ratios of ancient igneous rocks. In brief, they showed that in contrast to Archean samples, numerous Meso-Paleoproterozoic (1 to 2.5 billion years ago) subaerially erupted igneous rocks exist that are highly oxidized ($\text{Fe}^{3+}/\Sigma\text{Fe} > 0.4$) and attributed this oxidation to the presence of O_2 in the Proterozoic atmosphere, which began to accumulate starting ~ 2.5 to 2.3 billion years ago (e.g., refs. 5 and 11). As a specific example, greenschist metamorphic facies subaerial volcanic rocks from the 2,058-Ma Kuetsjärvi volcanic formation reach $\text{Fe}^{3+}/\Sigma\text{Fe} > 0.75$ (67). This shows that metamorphism does not universally lower $\text{Fe}^{3+}/\Sigma\text{Fe}$ ratios of ancient igneous rocks.

As our samples are submarine in origin, oxidation by atmospheric O_2 during eruption for extrusive samples is not an issue for our dataset, unlike for subaerial volcanic rocks. Stolper and Keller (10) also showed that the $\text{Fe}^{3+}/\Sigma\text{Fe}$ ratios of submarine basalts increase beginning between 541 to 420 Ma. They interpreted this as occurring due to the Phanerozoic oxygenation of the deep ocean carrying dissolved O_2 into hydrothermal systems circulating through oceanic crust—that is, due to oxidative alteration on the seafloor. Although large-scale hydrothermal circulation systems are best known from midocean-ridge and back-arc spreading centers, island arcs also create local hydrothermal cells (e.g., ref. 68). Consequently, the observed Phanerozoic increase in average submarine island arc rock $\text{Fe}^{3+}/\Sigma\text{Fe}$ ratios could be due to oxidation of submarine island arc igneous rocks by O_2 during hydrothermal circulation following the oxygenation of the deep ocean sometime between 800 and 400 Ma (e.g., refs. 1, 2, 4–6, and 10). We note, though, that the increase in Late Paleozoic–Cenozoic island arc rock $\text{Fe}^{3+}/\Sigma\text{Fe}$ ratios is approximately one-third of that seen in submarine basalts from ophiolites (10), indicating that hydrothermal circulation is unlikely to be the primary control on $\text{Fe}^{3+}/\Sigma\text{Fe}$ ratios of island arc igneous rocks.

Regardless, to test for time-variant subsolidus oxidation of the compiled samples during hydrothermal circulation, we compared $\text{Fe}^{3+}/\Sigma\text{Fe}$ ratios of intrusive vs. extrusive island arc igneous rocks from our compilation as a function of age (*SI Appendix*, Table S2). Modern extrusive rocks generally experience more oxidative alteration during hydrothermal circulation on the seafloor than intrusive rocks due to both their emplacement at Earth's surface and higher permeabilities; for example, hydrothermally altered

basalts from drilled oceanic crust and exposed ophiolite sequences and are typically elevated in $\text{Fe}^{3+}/\Sigma\text{Fe}$ by >0.2 compared with sheeted dykes and gabbros (e.g., refs. 69 and 70). Thus, extrusive rocks are expected to be more prone to hydrothermal oxidation on the seafloor than are intrusive rocks. Average $\text{Fe}^{3+}/\Sigma\text{Fe}$ for the Precambrian, Early Paleozoic, and Late Paleozoic–Cenozoic extrusive island arc rocks are 0.272 ± 0.022 (1 SE), 0.314 ± 0.030 , and 0.366 ± 0.023 , respectively. Average $\text{Fe}^{3+}/\Sigma\text{Fe}$ for intrusive island arc rocks for the same age ranges are 0.266 ± 0.028 , 0.245 ± 0.017 , and 0.425 ± 0.039 (*SI Appendix*, Fig. S4). Thus, for both the intrusive and extrusive groups, the Late Paleozoic–Cenozoic mean $\text{Fe}^{3+}/\Sigma\text{Fe}$ ratios for island arc rocks are greater (beyond 2 SE) than for the Precambrian samples. Additionally, the mean values for extrusive and intrusive rocks overlap at the 2 SE level for the specific age bins. Likewise, for the GEOROC island arc database (all Late Paleozoic or younger) the average $\text{Fe}^{3+}/\Sigma\text{Fe}$ ratios for extrusive and intrusive island arc rocks are 0.389 ± 0.015 (1 SE) and 0.361 ± 0.021 and thus within 2 SE of each other. Consequently, there appears to be no significant difference in average $\text{Fe}^{3+}/\Sigma\text{Fe}$ ratios between intrusive and extrusive island arc rocks through time for the given age ranges, and the observed increase in $\text{Fe}^{3+}/\Sigma\text{Fe}$ ratios with time is seen in both rock types. Finally, there is no apparent correlation between $\text{Fe}^{3+}/\Sigma\text{Fe}$ and the water content of the rocks (as given by the loss on ignition weight percent), indicating that hydrothermal alteration does not inherently promote oxidation or reduction of iron (*SI Appendix*, Fig. S5). Based on this, we infer that subsolidus oxidation during hydrothermal circulation of island arc rocks is not the cause of the observed difference in average $\text{Fe}^{3+}/\Sigma\text{Fe}$ of late Paleozoic–Cenozoic vs. Precambrian island arc rocks.

Changes in the degree of differentiation or degassing of island arc magmas with time.

Differentiation of a magma through fractional crystallization of minerals that preferentially incorporate Fe^{2+} over Fe^{3+} (e.g., olivine) will increase the $\text{Fe}^{3+}/\Sigma\text{Fe}$ value of a melt if a magma behaves as a closed system in regard to $f\text{O}_2$ (71–74). In contrast, crystallization and removal of Fe^{3+} -rich minerals (e.g., magnetite) from a melt will decrease the melt $\text{Fe}^{3+}/\Sigma\text{Fe}$ ratio (62, 75–77). We tested whether differences in the degree of fractionation has any control on the difference in mean $\text{Fe}^{3+}/\Sigma\text{Fe}$ ratios between the various age ranges by filtering samples based on their SiO_2 or MgO contents, where higher SiO_2 and lower MgO contents are indicative of greater differentiation. Even after removal of samples with >70 , 65 , and 60 wt % SiO_2 or $\text{MgO} <1$, 2 , 3 , 4 , and 5 wt %, mean $\text{Fe}^{3+}/\Sigma\text{Fe}$ values for the Precambrian vs. Late Paleozoic–Cenozoic do not overlap at the 2 SE level and change in value by at most 0.036 after filtering (*SI Appendix*, Table S1). This indicates that differences in degree of fractionation with time do not significantly influence the observed changes in $\text{Fe}^{3+}/\Sigma\text{Fe}$ ratios with time.

Degassing of a mixed H–C–O–S fluid can cause $\text{Fe}^{3+}/\Sigma\text{Fe}$ ratios of a melt to increase, decrease, or potentially not vary at all depending on which volatile

species are lost from the melt (e.g., refs. 57, 58, 62, and 78–82). For example, H₂ loss due to H₂O dissociation can increase melt fO_2 and thus Fe³⁺/ΣFe ratios (82) and has been called on as a potential explanation for the difference in Fe³⁺/ΣFe ratios of island arc basalts vs. MORB (33, 36). If a change in the amount of degassing of H₂O (or another volatile that causes the oxidation of residual melt) is the cause of the increase of Fe³⁺/ΣFe ratios of island arcs rocks in our compilation, then we would expect that this difference would be more pronounced in extrusive rocks, which experience more degassing than intrusive rocks. However, as already discussed, Fe³⁺/ΣFe ratios of intrusive vs. extrusive rocks for a given age range are similar and show a similar difference in Fe³⁺/ΣFe for Phanerozoic vs. Precambrian rocks. This indicates that the more oxidized nature of Phanerozoic vs. Precambrian island arc rocks is not due to a global change in the style of degassing in Phanerozoic vs. Precambrian island arc rocks.

Changes in the redox state of island arc mantle sources with time.

Given the above considerations, we propose that the increase in Fe³⁺/ΣFe ratios of island arc igneous rocks from the Precambrian to the Late Paleozoic (541 to 420 Ma) is primary. We further hypothesize that this increase results from changes in the fO_2 of the mantle sources of island arc magmas and consequently of primitive island arc rocks. This necessarily requires that the Fe³⁺/ΣFe ratios of island arc rocks primarily reflect the fO_2 of their mantle sources (e.g., refs. 22 and 24) as opposed to being controlled by oxidation/reduction during crystallization, ascent, and/or eruption (e.g., refs. 33 and 36). Additionally, this indicates that oxidizing fluids derived from subducted serpentinitized ultramafic rocks do not fully control the redox budget of the subarc mantle as otherwise Fe³⁺/ΣFe ratios of island arc rocks of all ages should be elevated. This presumes there were not large-scale changes around the Precambrian–Cambrian boundary in rates of serpentinitization or how serpentinite-derived oxidants are transferred to the subarc mantle—we are unaware of any evidence for such a change.

Below we propose that the Phanerozoic increase in Fe³⁺/ΣFe ratios of island arc igneous rocks is due to increased dissolved O₂ and sulfate concentrations in the deep ocean 800 to 400 Ma. The higher O₂ and sulfate concentrations increased the redox state of sediments and hydrothermally altered oceanic crust that is eventually subducted to the subarc mantle, oxidizing it and, as a result, increasing the fO_2 of the parental melts of island arc rocks (10, 18, 19). We additionally comment below on the observed scatter in average locality Fe³⁺/ΣFe ratios observed in light of this proposal. Before discussing this further, we first explore an obvious prediction of our proposal: If the increase in Fe³⁺/ΣFe does indeed represent an increase in the fO_2 of the subarc mantle, then other redox-sensitive parameters that can track the fO_2 of island arc igneous rocks should also increase over this same time period. In the next section we evaluate whether this is the case for the widely used V/Sc oxybarometer before exploring the geological implications of the compiled records further below.

V/Sc Ratios of Island Arc Rocks Through Time.

An alternative parameter to $\text{Fe}^{3+}/\Sigma\text{Fe}$ ratios commonly used to track the $f\text{O}_2$ of a mantle source and its partial melts is the whole-rock V/Sc ratio (32, 33). Specifically, as the $f\text{O}_2$ of a peridotite source increases, the V/Sc ratio increases in a partial melt due to the increased bulk incompatibility of V as its oxidation state increases (34, 83). In contrast to $\text{Fe}^{3+}/\Sigma\text{Fe}$ ratios, V/Sc ratios of igneous rocks have been argued to be largely impervious to low-temperature alteration, metamorphism, and the effects of differentiation and degassing for high-MgO rocks (32, 33). Although V/Sc ratios of basalts are also sensitive to degree of partial melting and the initial V/Sc ratio of their mantle source (32, 33, 84), if these parameters are roughly constant through time for island arc magmatism, then V/Sc ratios of island arc rocks are expected to be sensitive to variations in the $f\text{O}_2$ of a peridotitic source. Thus, to complement and further test the significance of the $\text{Fe}^{3+}/\Sigma\text{Fe}$ -ratio record, we also compiled V/Sc ratios of island arc igneous rocks from the past 3.1 billion years.

In Fig. 2, we provide the mean V/Sc value of each island arc locality as a function of age as well as the average value for of all localities from a given age range. Data histograms are given in *SI Appendix*, Fig. S6. Here we have combined our compilation of Late Paleozoic–Cenozoic island arc samples with those of the GERO database (which cover the same time frame) to increase data coverage from the Late Paleozoic to Cenozoic. We also provide average V/Sc ratios of modern MORB based on mean values at a given plate boundary, 6.83 ± 0.10 (1 SE; data from ref. 55), which is in agreement with that given by Li and Lee (32) of 6.74. Additionally, we present measurements of V/Sc ratios of Precambrian basalts previously used to reconstruct the $f\text{O}_2$ of the upper mantle (Fig. 2 and refs. 32 and 35). These yield a mean V/Sc ratio of 6.38 ± 0.24 (1 SE), within 2 SE of modern MORB. This lack of a discernible change in V/Sc in nonsubduction related basalts is consistent with previous studies that found no clear change in the $f\text{O}_2$ of the magma-producing upper mantle potentially from the Archean or at least Proterozoic (2.5 billion years ago) to today (32, 35, 85, 86). Note that we have not included V/Sc ratios of eclogites (35) or komatiites (85) used to reconstruct past mantle $f\text{O}_2$ values given their different formational environments, degrees of melting, and metamorphic histories compared with typical basalts. Such rocks potentially indicate lower (~ 1 log unit) mantle $f\text{O}_2$ values compared with modern before 2.5 billion years ago (35), but similar mantle $f\text{O}_2$ values from the Proterozoic on (2.5 to 0 billion years ago; refs. 35 and 86).

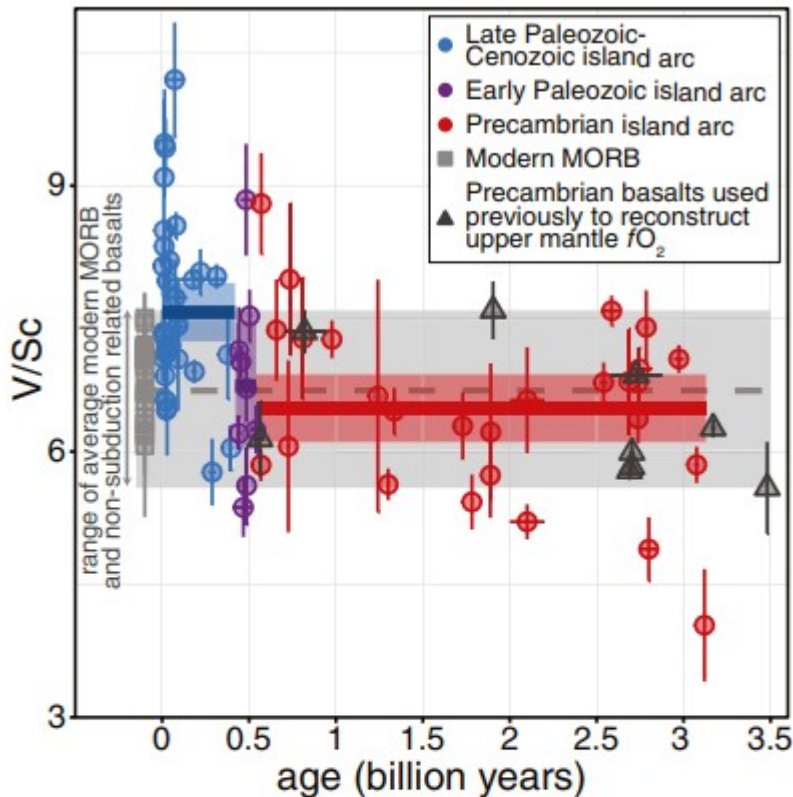


Fig. 2. Average V/Sc ratios of island arc rocks through time. Each data point is the average value of a specific island arc locality. Data include both intrusive and extrusive igneous rocks. Solid horizontal lines are averages of the formational means over the given time period: 6.49 ± 0.19 (1 SE) for the Precambrian, 6.74 ± 0.35 for the Early Paleozoic, and 7.57 ± 0.17 for the Late Paleozoic–Cenozoic. Shading represents 2 SE. Vertical error bars for individual points are 1 SE. Horizontal age uncertainties vary depending on the age constraints available for each island arc (Dataset S1). The gray horizontal bar is the V/Sc range of the averages of modern MORB for specific plate boundaries (from ref. 55) and ancient basalts used previously to reconstruct past upper mantle fO_2 (data from refs. 32 and 35): average of 6.69 and range of 5.59 to 7.59.

In contrast, mean V/Sc ratios of the island arc localities using the same age ranges as for the $Fe^{3+}/\Sigma Fe$ ratios are 6.49 ± 0.19 (1 SE; 27 locations, 307 analyses) for the Precambrian, 6.74 ± 0.35 (9 locations, 129 analyses) for the Early Paleozoic, and 7.57 ± 0.17 (11 locations compiled by us and 24 from GEOROC, 98 analyses compiled by us and 2,855 from GEOROC) for the Late Paleozoic–Cenozoic. The average V/Sc ratio for the Late Paleozoic–Cenozoic differs significantly ($P < 0.05$) from that of the Precambrian ($P = 0.0008$; Tukey’s honestly significant difference test), while the Early Paleozoic mean is neither statistically distinct ($P > 0.05$) from the Late Paleozoic–Cenozoic mean ($P = 0.10$) nor the Precambrian mean ($P = 0.95$). Use of a 6.5 wt % MgO filter does not control the result: Late Paleozoic–Cenozoic island arc rock V/Sc ratios are elevated relative to Precambrian

island arc rocks by 1.08 using an MgO filter of 6.5 wt % and by 1.20 using a filter of 8.0 wt %. Finally, our average V/Sc ratio for the Late Paleozoic–Cenozoic time period (7.57 ± 0.17) is within 0.12 of the value for similarly aged island arc volcanic rocks independently compiled in Turner and Langmuir (87) of 7.69 ± 0.28 (1 SE) when an MgO filter of 6.5 to 15 wt % is applied to that data. Again, we examined the fidelity of choice of our age bins by fitting a moving average data to the data (*SI Appendix*, Fig. S7). As was the case for the $\text{Fe}^{3+}/\Sigma\text{Fe}$ ratio, this approach shows an increase in V/Sc ratios after 541 Ma, and is thus consistent with our analysis above.

An increase of ~ 1 in the V/Sc ratio corresponds to an increase in ~ 0.5 log units of $f\text{O}_2$ at 10 to 20% partial melting of a spinel lherzolite with V and Sc contents the same as that for the source of MORB (32, 33). Some Cenozoic localities, however, record average V/Sc values of 9 to 10, which could correspond to an increase in $f\text{O}_2$ of a log unit or more at similar melting conditions. Thus, like the $\text{Fe}^{3+}/\Sigma\text{Fe}$ ratios, the V/Sc ratios are consistent with a statistically significant increase in the redox state of island arc mantle sources and primary melts from the Neoproterozoic to Phanerozoic. Importantly, this increase does not appear to occur in nonisland arc basalts and is instead specific to island arc rocks (Fig. 2). Additionally, we note that our compilation and that of ref. 87 yield average V/Sc ratios of modern island arc rocks that are elevated vs. MORB by ~ 0.8 (and differ beyond 2 SE)—this is in contrast to previous work that argued for no significant difference between the two (33, 34). If the elevation in V/Sc observed here between modern island arcs and MORB is interpreted following typical frameworks (32–34), then it would indicate the source of island arc rocks is more oxidized (higher $f\text{O}_2$) relative to the source of MORB. If correct, then the V/Sc and $\text{Fe}^{3+}/\Sigma\text{Fe}$ ratios of island arc rocks and MORB are actually in qualitative agreement on this issue (22, 24, 58, 59).

In *SI Appendix*, Fig. S8 we directly compare V/Sc vs. $\text{Fe}^{3+}/\Sigma\text{Fe}$ ratios of time period means and locality averages. Linear regressions of both yield a positive correlation, as would be expected. This direct comparison of V/Sc and $\text{Fe}^{3+}/\Sigma\text{Fe}$ ratios is complicated by two issues. First, only one-third of the non-GEOROC localities have both $\text{Fe}^{3+}/\Sigma\text{Fe}$ and V/Sc ratios available, and most (92%) of the V/Sc and $\text{Fe}^{3+}/\Sigma\text{Fe}$ measurements in our compilation are not on the same samples. Thus, a clear area of future work is a direct comparison of $\text{Fe}^{3+}/\Sigma\text{Fe}$ vs. V/Sc measured on the same samples for Precambrian vs. Phanerozoic aged rocks.

Second, although both V/Sc and $\text{Fe}^{3+}/\Sigma\text{Fe}$ ratios in partial melts of the mantle are sensitive to source $f\text{O}_2$, the exact dependence of V/Sc on $f\text{O}_2$ is a function of the degree of melting (33, 84), modal mineralogy of the source (33), and the initial V/Sc ratio of the source (84). Lower initial V/Sc ratios of the subarc mantle due to prior melt extraction (e.g., from back-arc spreading centers) has recently been proposed to strongly influence the relationship between V/Sc ratios of arc basalts and the $f\text{O}_2$ of the source region (84). We explored this issue quantitatively by modeling V and Sc partitioning during partial

melting of the mantle (*SI Appendix*). We examined how V/Sc vs. $\text{Fe}^{3+}/\Sigma\text{Fe}$ ratios vary for a primitive basalt given plausible ranges in source $f\text{O}_2$, source V/Sc, modal mineralogy, and melt fraction (*SI Appendix*, Fig. S9). In *SI Appendix*, Fig. S10 we overlay the potential modeled ranges of V/Sc vs. $\text{Fe}^{3+}/\Sigma\text{Fe}$ on our compiled data corrected for an increase in 0.074 in $\text{Fe}^{3+}/\Sigma\text{Fe}$ ratios due to later oxidation (as based on the XANES comparison above). All data fall within a modeled $f\text{O}_2$ range of -1 to 4 log units below or above QFM, a typical range for MORB and island arc sources (21, 22, 29, 58, 59). This shows that our measured V/Sc and $\text{Fe}^{3+}/\Sigma\text{Fe}$ are reasonable and in agreement. Our model reinforces the conclusion of ref. 84 that the precise relationship between V/Sc and melt $f\text{O}_2$ is model-dependent.

We expect that the generation of island arcs has been similar through time (similar degrees of melt and similar amount of prior melt depletion), and as such that V/Sc ratios can be used to track relative changes in the $f\text{O}_2$ of island arc sources with time. Based on this, we propose the observed increase in V/Sc ratios to be most simply interpreted to reflect an increase in the $f\text{O}_2$ of the subarc mantle sometime between the end of the Neoproterozoic through to the early Paleozoic. Most importantly, this is in agreement with and provides strong independent evidence for our interpretation of the $\text{Fe}^{3+}/\Sigma\text{Fe}$ data as reflecting an increase in the redox state of the subarc mantle between 800 and 400 Ma.

Finally, we also examined V/Yb ratios for our compilation as this ratio has independently been proposed to be a oxybarometer (37). We observe a hyperbolic relationship between V/Yb vs. Yb (*SI Appendix*, Fig. S11) such that at lower (<2 ppm) Yb concentrations V/Yb ratios are clearly elevated relative to samples with higher (>2 ppm) Yb concentrations. We expect that this hyperbolic relationship derives, in part, from imprecisions and inaccuracies in Yb measurements such that at the already low Yb concentrations [most (62%) samples have <2 ppm Yb] small (<0.5 ppm) measurement errors generate the hyperbolic relationship. Given this complexity (which is not present in the V/Sc dataset; *SI Appendix*, Fig. S11) we do not apply the V/Yb oxybarometer to our dataset.

Porphyry Copper Deposits.

It has been proposed that oxidized arc melts (relative to MORB) are a necessary condition for the generation of porphyry copper deposits commonly associated with island and especially continental arcs (25, 88), although this is debated (e.g., ref. 41). Porphyry copper deposits in the Precambrian are rare and a rise in their occurrence begins at the start of the Phanerozoic (89) coinciding with the increase in $\text{Fe}^{3+}/\Sigma\text{Fe}$ and V/Sc ratios of the island arc compilation presented here (Fig. 3 A-C). Some have ascribed this increase to a bias in the rock record in which preferential erosional loss of Precambrian deposits has occurred (90). Alternatively both Evans and Tomkins (18) and Richards and Mumin (19) proposed that the Phanerozoic increase is a primary feature of the rock record and that the increase is due

to the oxygenation of the deep ocean, which increased marine sulfate concentrations, which in turn led to an increase in both the sulfur content and redox state of arc parental melts via subduction and incorporation of this sulfate into the subarc mantle. The key point is that although the formation (91) and preservation of porphyry copper deposits is potentially complex their temporal record is consistent with and has previously and independently been linked to the idea of a Phanerozoic increase in the redox state of the mantle source of island arc magmas as we have proposed here.

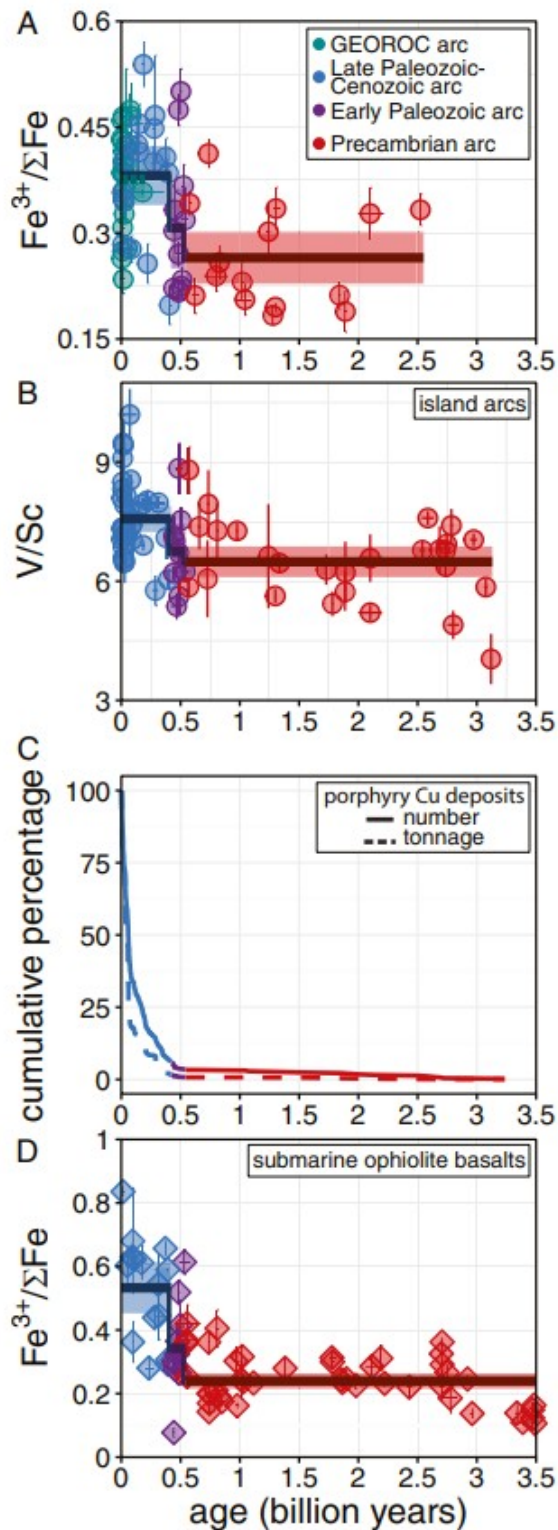


Fig. 3. Parameters associated with changes in the redox state of island arc rocks with time. (A) $Fe^{3+}/\Sigma Fe$ ratios of island arc rocks through time as in Fig. 1. (B) V/Sc ratios of island arc rocks through time as in Fig. 2. (C) Abundance of porphyry copper deposits with time (data from ref. 89). (D) $Fe^{3+}/\Sigma Fe$ ratios of submarine basalts from ophiolites through time indicative of the redox state of altered oceanic crust (data from ref. 10).

Effects of Deep-Ocean O₂ and Marine Sulfate Concentrations on the fO_2 of Island Arc Mantle Sources.

Based on the island arc $Fe^{3+}/\Sigma Fe$ and V/Sc records and the temporal distribution of porphyry copper deposits, we propose an increase in the redox state of the mantle source of island arcs occurred sometime between the end of the Neoproterozoic and the Early Paleozoic. The question is, what geological process (or processes) drove this change? As discussed, a leading hypothesis for why modern igneous island arc rocks are more oxidized vs. MORB is that oxidized material from the subducted slab is transferred to and thus oxidizes the subarc mantle, which melts to form island arc rocks. Thus, an increase in the redox state of subducted oceanic crust from the Neoproterozoic to Early Phanerozoic provides a plausible explanation for the observed increase in the redox state of island arcs over this time frame.

Over the same time interval that our compilation indicates that island arc magmas became more oxidized (800 to 400 Ma), the atmosphere is thought to have accumulated sufficient O₂ (10 to 50% of modern) to oxygenate the majority of the deep oceans (e.g., refs. 1–10). Additionally, marine sulfate concentrations are thought to have also increased to near modern levels over this same time frame (e.g., refs. 13–17). Based on this, we propose that this oxygenation and elevation in marine sulfate concentrations increased the redox state of altered oceanic crust that, when eventually subducted to the mantle, oxidized the mantle source of island arc rocks.

There are at least three ways the oxygenation of the deep ocean and an increase in marine sulfate concentrations could have increased the redox state of subducted oceanic crust. (i) Deep ocean oxygenation would have increased the redox state of deep-sea sediments by increasing sedimentary $Fe^{3+}/\Sigma Fe$ ratios and potentially lowering organic carbon contents (burial of organic carbon is enhanced in anoxic vs. oxic settings; e.g., ref. 92). (ii) Circulation of O₂ derived from deep ocean waters would have oxidized iron and sulfur in oceanic crust—indeed, $Fe^{3+}/\Sigma Fe$ ratios of submarine basalts from ophiolites show a threefold increase from the Neoproterozoic to Late Paleozoic–Cenozoic (Fig. 3D and ref. 10). This independently demonstrates that there was an increase in the redox state of altered oceanic basalts over the same time frame the redox state of island arc rocks increases. (iii) Increased dissolved sulfate levels in the ocean could have increased the redox state of subducted oceanic crust at this time (18, 19) either during high-temperature (>150 °C) hydrothermal circulation with anhydrite precipitation (if anhydrite does not redissolve before subduction; refs. 93 and 94) and/or oxidation of Fe^{2+} -bearing minerals by sulfate, which occurs in experiments at elevated (>200 °C) temperatures (95). Which of these processes is most important in causing the observed increase in island arc redox state is not clear, and it is possible, and perhaps likely, that all played a role—in other words, our record does not identify the oxidant (Fe^{3+} vs. sulfate) or source of the oxidant (sediments vs. altered igneous rocks) of the subarc mantle. A schematic cartoon of how changes in deep-

ocean O_2 and sulfate concentrations with time could have influenced the redox state of island arc rocks is given in Fig. 4. We note that we have not considered changes in carbonate subduction fluxes with time as it has been argued that subducted carbonate is not a source of oxidants for island-arc melts (18) because at the depths that these melts are derived (≈ 120 km), carbon exists as C^{4+} in carbonate or CO_2 (96). However, if these melts formed at greater depths where graphite is stable, subducted carbonate could oxidize the subarc mantle (40).

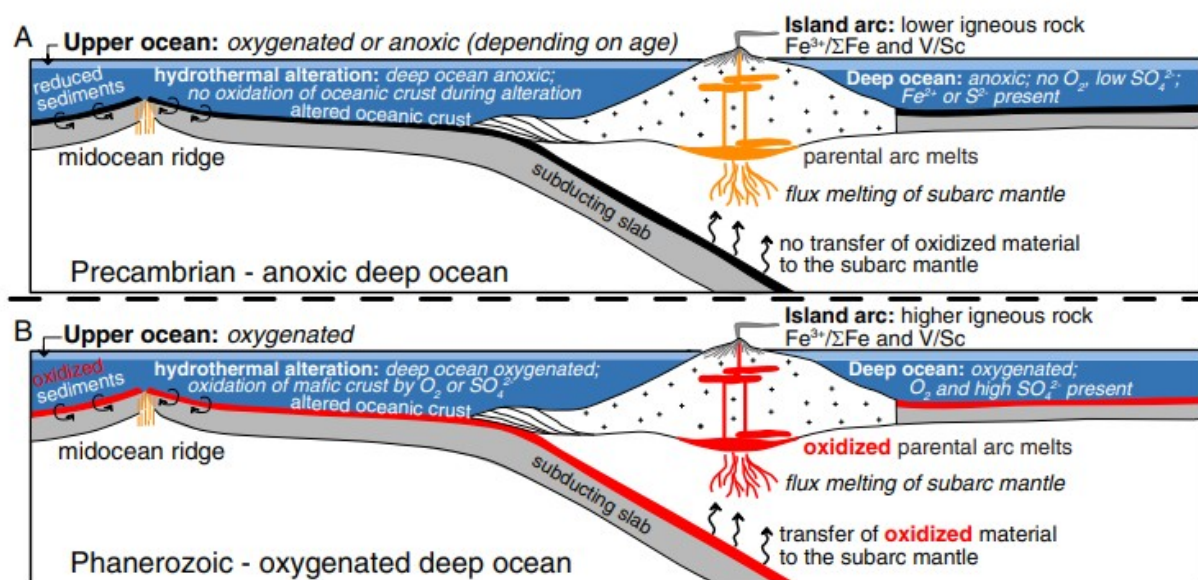


Fig. 4. (A and B) Schematic cartoon of how proposed changes in the redox state of the deep ocean alters the redox state of igneous island arc rocks.

For our given age bins, there is significant scatter in $Fe^{3+}/\Sigma Fe$ and V/Sc values (Figs. 1 and 2). For example, although most Late Paleozoic–Cenozoic samples are more oxidized than Precambrian equivalents, some Late Paleozoic–Cenozoic localities are lower in $Fe^{3+}/\Sigma Fe$ and V/Sc than the average value for the Precambrian. Some of this scatter likely results from alteration of some samples or methodological differences for the measurement of FeO and Fe_2O_3 wt % or V and Sc abundances between studies. However, it not expected that there should by a single value for $Fe^{3+}/\Sigma Fe$ or V/Sc ratios of island arc rocks for a given age range once subduction of oxidized material begins. This is because the extent of subarc oxidation during subduction has been proposed to be controlled by the age of the arc, the total amount of oceanic crust subducted, and convergence rate, all of which influence the integrated flux of oxidants to a subduction zone and the ability of those oxidants to be released at depth and infiltrate the subarc mantle vs. escape up the slab–mantle interface (29). Thus, based on previous work (29), records of $Fe^{3+}/\Sigma Fe$ and V/Sc ratios from similarly aged island arc localities are expected to show a range of values.

The $Fe^{3+}/\Sigma Fe$ and V/Sc records are unlikely to be able to provide a definitive estimate of when precisely the deep ocean became oxygenated or

experienced increased sulfate concentrations given both the scatter in the records and the inherent lag of potentially up to $\sim 10^8$ years between when oceanic crust becomes oxidized on the seafloor, when it is subducted and releases these oxidants to the subarc mantle, when the subarc melts, and when those melts erupt and crystallize to form island arc rocks. For example, Evans and Tomkins (18) estimated that for an oxygenated deep ocean 2.4×10^{12} mol/y of oxidants are subducted. This combined with assumptions about how material is transferred from the slab to the subarc mantle and mantle mixing rates, they (18) modeled that it takes between 10^4 and 10^7 years to noticeably (>0.3 log unit change in fO_2) oxidize the subarc mantle and that it takes 10^6 to 10^8 years for the subarc mantle to reach a steady state fO_2 of 1 to 3 log units above the MORB source. This does not account for the $\sim 10^7$ years needed to oxidize the oceanic crust on the seafloor.

Additionally, although a rise in both marine seawater sulfate (e.g., refs. 13–17) and deep-ocean O_2 concentrations (e.g., refs. 1, 2, 4–6, and 10) are thought to have occurred toward the end of the Neoproterozoic through the early Phanerozoic, whether these occurred simultaneously is not known. Thus, an increase in marine sulfate levels could predate and cause the oxidation of the subarc mantle by sulfate (in part or fully) before the oxygenation of the deep ocean. Regardless, the presented island arc record is broadly consistent with independent work that indicates the deep oceans were anoxic and relatively sulfate-poor (compared with modern) before the Neoproterozoic ($>1,000$ Ma), and that permanent deep-ocean oxygenation and sulfate accumulation occurred sometime during or after the Neoproterozoic (1, 2, 4–6, 8, 10, 12–17, 97). We note that atmospheric O_2 and marine sulfate levels are proposed to have temporarily reached near modern levels ~ 2 billion years ago (in the aftermath of the initial oxygenation of the atmosphere) before subsiding back to lower values within $\sim 10^8$ years (98, 99). Our data compilation lacks the temporal resolution needed to test whether any oxidation of the subarc mantle occurred due to subduction of oxidized material generated during this brief excursion in O_2 and sulfate levels.

So far, we have focused on how the oxygenation of the deep ocean and the associated increase in marine sulfate concentrations could have led to an increase in the fO_2 of mantle sources of island arc magmas. However, it is worth speculating on how the redox state of subducted oceanic crust could have differed in the Precambrian when the ocean is thought to have been anoxic with either Fe^{2+} or sulfide as the main redox-active dissolved species (5, 11, 97, 100). Anoxic deep oceans could have led to an increase in the relative amount of organic carbon reaching sediments vs. that sinking out of the mixed layer of the ocean (e.g., ref. 92) as well as a decrease in the $Fe^{3+}/\Sigma Fe$ ratio of Fe in deep-sea sediments. Additionally, dissolved Fe^{2+} or sulfide in the deep ocean could have been fixed in altered oceanic basalts during hydrothermal alteration as iron-rich clays or sulfide minerals (e.g., pyrite). If sufficient organic carbon and/or Fe^{2+} and reduced sulfur-bearing

minerals were sequestered in sediments or altered oceanic crust, subduction of oceanic crust could have actually reduced the subarc mantle in the Precambrian before the oxygenation of the deep ocean.

Although speculative, this idea is consistent with the data presented here. The V/Sc ratios of some Precambrian (and particularly Mesoproterozoic and older) island arc rocks are lower than those for modern MORB (Fig. 2), potentially indicative of a more reduced source for island arc parental melts. We note that there is another potential explanation for the lower V/Sc ratios of some Mesoproterozoic and older island arc rocks vs. modern MORB. Specifically, a depleted mantle source for island arc parental melts has been proposed to lower the initial V/Sc of the mantle source for modern island arcs (84). Without the compensatory effect of oxidized material in the subducted slabs to increase the subarc mantle fO_2 (and thus raise the V/Sc ratio of the island arc parental melts), this prior melt depletion could have acted to lower the V/Sc ratios of Mesoproterozoic and older island arc rocks. Whether the subduction of reduced altered oceanic crust vs. source depletion controls the V/Sc ratios of Mesoproterozoic and older island arc rocks is unclear. Importantly, both are consistent with an increase in the flux of oxidized material subducted to the subarc mantle causing an increase in V/Sc ratios of island arc rocks as we have proposed here.

Implications for the Formation of Calc-Alkaline Rocks.

As parental melts of MORB crystallize, total iron contents increase forming the “tholeiitic” or “iron-enrichment” trend (e.g., refs. 73, 101, and 102), whereas in some island, and especially continental, arc magmas, total iron contents remain constant or decrease as melts differentiate, following the “iron-depletion” or “calc-alkaline” trend (e.g., refs. 102 and 103). One explanation for these different trends is that the elevated fO_2 of arc magmas results in spinels rich in the Fe^{3+} -bearing magnetite component to saturate early during crystallization, extracting significant iron from the melt and preventing iron enrichment (e.g., refs. 20 and 71). Importantly, Archean and early Proterozoic igneous rocks exist that follow the calc-alkaline trend (e.g., refs. 104 and 105). Additionally, it has recently been argued that the ratio of tholeiitic vs. calc-alkaline rocks preserved in continental crust has not changed over the past ~ 3.8 billion years (45). As the $Fe^{3+}/\Sigma Fe$ and V/Sc compilations suggest that the fO_2 of Precambrian island arcs and MORB mantle sources were similar (Fig. 2), it must follow, according to the hypothesis developed here, that an elevated fO_2 of island arc sources (and thus continental arc sources as well) relative to MORB sources is not an essential ingredient in the generation of calc-alkaline rocks characterized by suppression of iron enrichment during crystallization. Instead, other explanations for the calc-alkaline trend, such as the elevated water contents of the mantle sources of primitive island arc magmas (e.g., refs. 106 and 107), must also be important in creating iron-depletion trends in Precambrian arc rocks.

Conclusions

In previous discussions of the evolution of the redox state of the mantle and ocean/atmosphere, a focus has been on how changes in the fO_2 of the mantle could (or could not) have caused the initial rise in atmospheric O_2 levels ~2.4 to 2.3 billion years ago via the control of mantle fO_2 on the redox state of volcanic gasses emitted to the atmosphere (e.g., refs. 32, 35, 61, 64, 108, and 109). We interpret the results presented here to indicate that the opposite is the case for the later rise of atmospheric O_2 sometime between 800 to 400 Ma to near-modern (10 to 50%) levels and the associated rise in marine sulfate concentrations. Over this time period, rather than changes in mantle fO_2 controlling the redox state of the atmosphere and ocean, we propose that changes in the redox state of the atmosphere and deep ocean influenced the fO_2 of the subarc mantle (i.e., the source region of island arc melts) through subduction of oceanic crust that was oxidized via interaction with an oxygenated deep ocean with elevated sulfate concentrations. This in turn led to an increase in the redox state of island arc magmas, which are the building blocks of new continental crust. This represents a rare example of changes in the biogeochemistry of Earth's surface leading to significant changes in the geochemical evolution of the mantle and the chemical composition of an important class of igneous rocks. Finally, by using ancient island arc rocks and taking advantage of the change in the boundary conditions of the redox state of the deep oceans through time, this work presents independent and distinct evidence that the more oxidized nature of modern igneous island arc rocks vs. MORB is derived from the transfer of oxidized material in the subducted slab from sediments or altered mafic crust to the subarc mantle as opposed to serpentinization of subducted slabs or processes associated with transit of magmas through the crust and eruption.

Acknowledgments

We thank E. Cottrell, M. Hirshmann, and E. Stolper for helpful discussions; Z. Brook for help compiling the data; J. Blundy and C. Langmuir for feedback on an earlier draft; and M. Brounce and L. Kump for constructive reviews.

Footnotes

1 To whom correspondence may be addressed.
Email: dstolper@berkeley.edu or cbucholz@caltech.edu.

References

1. Canfield DE, Poulton SW, Narbonne GM (2007) Late-Neoproterozoic deep-ocean oxygenation and the rise of animal life. *Science* 315:92–95.
2. Dahl TW, et al. (2010) Devonian rise in atmospheric oxygen correlated to the radiations of terrestrial plants and large predatory fish. *Proc Natl Acad Sci USA* 107: 17911–17915.
3. Shields-Zhou G, Och L (2011) The case for a Neoproterozoic oxygenation event: Geochemical evidence and biological consequences. *GSA Today* 21:4–11.
4. Sahoo SK, et al. (2012) Ocean

oxygenation in the wake of the Marinoan glaciation. *Nature* 489:546–549. 5. Lyons TW, Reinhard CT, Planavsky NJ (2014) The rise of oxygen in Earth's early ocean and atmosphere. *Nature* 506:307–315. 6. Sperling EA, et al. (2015) Statistical analysis of iron geochemical data suggests limited late Proterozoic oxygenation. *Nature* 523:451–454. 7. Blamey NJ, et al. (2016) Paradigm shift in determining Neoproterozoic atmospheric oxygen. *Geology* 44:651–654. 8. Lenton TM, et al. (2016) Earliest land plants created modern levels of atmospheric oxygen. *Proc Natl Acad Sci USA* 113:9704–9709. 9. Wallace MW, Shuster A, Greig A, Planavsky NJ, Reed CP (2017) Oxygenation history of the Neoproterozoic to early Phanerozoic and the rise of land plants. *Earth Planet Sci Lett* 466:12–19. 10. Stolper DA, Keller CB (2018) A record of deep-ocean dissolved O₂ from the oxidation state of iron in submarine basalts. *Nature* 553:323–327. 11. Canfield DE (2005) The early history of atmospheric oxygen: Homage to Robert M. Garrels. *Annu Rev Earth Planet Sci* 33:1–36. 12. Planavsky NJ, et al. (2014) Earth history. Low mid-Proterozoic atmospheric oxygen levels and the delayed rise of animals. *Science* 346:635–638. 13. Kah LC, Lyons TW, Frank TD (2004) Low marine sulphate and protracted oxygenation of the Proterozoic biosphere. *Nature* 431:834–838. 14. Canfield DE, Farquhar J (2009) Animal evolution, bioturbation, and the sulfate concentration of the oceans. *Proc Natl Acad Sci USA* 106:8123–8127. 15. Lyons TW, Gill BC (2010) Ancient sulfur cycling and oxygenation of the early biosphere. *Elements* 6:93–99. 16. Algeo TJ, Luo GM, Song HY, Lyons TW, Canfield DE (2015) Reconstruction of secular variation in seawater sulfate concentrations. *Biogeosciences* 12:2131–2151. 17. Turner EC, Bekker A (2016) Thick sulfate evaporite accumulations marking a midNeoproterozoic oxygenation event (Ten Stone Formation, Northwest Territories, Canada). *GSA Bulletin* 128:203–222. 18. Evans K-A, Tomkins A-G (2011) The relationship between subduction zone redox budget and arc magma fertility. *Earth Planet Sci Lett* 308:401–409. 19. Richards JP, Mumin AH (2013) Magmatic-hydrothermal processes within an evolving Earth: Iron oxide-copper-gold and porphyry Cu±Mo±Au deposits. *Geology* 41: 767–770. 20. Gill JB (1981) *Orogenic Andesites and Plate Tectonics* (Springer, New York). 21. Ballhaus C, Berry RF, Green DH (1990) Oxygen fugacity controls in the Earth's upper mantle. *Nature* 348:437–440. 22. Carmichael IS (1991) The redox states of basic and silicic magmas: A reflection of their source regions? *Contrib Mineral Petrol* 106:129–141. 23. Lécuyer C, Ricard Y (1999) Long-term fluxes and budget of ferric iron: Implication for the redox states of the Earth's mantle and atmosphere. *Earth Planet Sci Lett* 165: 197–211. 24. Kelley KA, Cottrell E (2009) Water and the oxidation state of subduction zone magmas. *Science* 325:605–607. 25. Mungall JE (2002) Roasting the mantle: Slab melting and the genesis of major Au and Au-rich Cu deposits. *Geology* 30:915–918. 26. Arculus RJ (1985) Oxidation status of the mantle: Past and present. *Annu Rev Earth Planet Sci* 13:75–95. 27. Wood BJ, Bryndzia LT, Johnson KE (1990) Mantle oxidation state and its relationship to tectonic environment and fluid speciation. *Science* 248:337–345. 28. Parkinson IJ, Arculus RJ (1999) The redox state of subduction zones: Insights from arc-

peridotites. *Chem Geol* 160:409–423. 29. Evans K, Elburg M, Kamenetsky V (2012) Oxidation state of subarc mantle. *Geology* 40:783–786. 30. Bénard A, et al. (2018) Oxidising agents in sub-arc mantle melts link slab devolatilisation and arc magmas. *Nat Commun* 9:3500. 31. Christie DM, Carmichael IS, Langmuir CH (1986) Oxidation states of mid-ocean ridge basalt glasses. *Earth Planet Sci Lett* 79:397–411. 32. Li Z-XA, Lee C-TA (2004) The constancy of upper mantle fO_2 through time inferred from V/Sc ratios in basalts. *Earth Planet Sci Lett* 228:483–493. 33. Lee C-TA, Leeman WP, Canil D, Li Z-XA (2005) Similar V/Sc systematics in MORB and Arc basalts: Implications for the oxygen fugacities of their mantle source regions. *J Petrol* 46:2313–2336. 34. Mallmann G, O'Neill HSC (2009) The crystal/melt partitioning of V during mantle melting as a function of oxygen fugacity compared with some other elements (Al, P, Ca, Sc, Ti, Cr, Fe, Ga, Y, Zr and Nb). *J Petrol* 50:1765–1794. 35. Aulbach S, Stagno V (2016) Evidence for a reducing Archean ambient mantle and its effects on the carbon cycle. *Geology* 44:751–754. 36. Lee C-TA, et al. (2010) The redox state of arc mantle using Zn/Fe systematics. *Nature* 468:681–685. 37. Laubier M, Grove TL, Langmuir CH (2014) Trace element mineral/melt partitioning for basaltic and basaltic andesitic melts: An experimental and laser ICP-MS study with application to the oxidation state of mantle source regions. *Earth Planet Sci Lett* 392:265–278. 38. Sobolev AV, et al. (2016) Komatiites reveal a hydrous Archean deep-mantle reservoir. *Nature* 531:628–632. 39. Alt JC, et al. (2012) Recycling of water, carbon, and sulfur during subduction of serpentinites: A stable isotope study of Cerro del Almirez, Spain. *Earth Planet Sci Lett* 327:50–60. 40. Evans KA (2012) The redox budget of subduction zones. *Earth Sci Rev* 113:11–32. 41. Lee C-TA, et al. (2012) Copper systematics in arc magmas and implications for crustmantle differentiation. *Science* 336:64–68. 42. Dauphas N, et al. (2009) Iron isotopes may reveal the redox conditions of mantle melting from Archean to Present. *Earth Planet Sci Lett* 288:255–267. 43. Ulmer P, Kaegi R, Müntener O (2018) Experimentally derived intermediate to silicarich arc magmas by fractional and equilibrium crystallization at 1.0 GPa: An evaluation of phase relationships, compositions, liquid lines of descent and oxygen fugacity. *J Petrol* 59:11–58. 44. Hawkesworth C, Cawood PA, Dhuime B (2018) Rates of generation and growth of the continental crust. *Geosci Front* 10:165–173. 45. Keller B, Schoene B (2018) Plate tectonics and continental basaltic geochemistry throughout Earth history. *Earth Planet Sci Lett* 481:290–304. 46. Pearce JA, Cann JR (1973) Tectonic setting of basic volcanic rocks determined using trace element analyses. *Earth Planet Sci Lett* 19:290–300. 47. Perfit MR, Gust DA, Bence AE, Arculus RJ, Taylor SR (1980) Chemical characteristics of island-arc basalts: Implications for mantle sources. *Chem Geol* 30:227–256. 48. Pearce JA, Peate DW (1995) Tectonic implications of the composition of volcanic arc magmas. *Annu Rev Earth Planet Sci* 23:251–285. 49. Hawkins JW, Bloomer SH, Evans CA, Melchior JT (1984) Evolution of intra-oceanic arc-trench systems. *Tectonophysics* 102:175–205. 50. Stern RJ, Morris J, Bloomer SH, Hawkins JW, Jr (1991) The source of the subduction component in

convergent margin magmas: Trace element and radiogenic isotope evidence from eocene boninites, Mariana forearc. *Geochim Cosmochim Acta* 55: 1467–1481. 51. Furnes H, Dilek Y, De Wit M (2015) Precambrian greenstone sequences represent different ophiolite types. *Gondwana Res* 27:649–685. 52. Safonova I, Kotlyarov A, Krivonogov S, Xiao W (2017) Intra-oceanic arcs of the PaleoAsian ocean. *Gondwana Res* 50:167–194. 53. Woodhead J, Eggins S, Gamble J (1993) High field strength and transition element systematics in island arc and back-arc basin basalts: Evidence for multi-phase melt extraction and a depleted mantle wedge. *Earth Planet Sci Lett* 114:491–504. 54. Kushiro I (1969) The system forsterite-diopside-silica with and without water at high pressures. *Am J Sci* 267:269–294. 55. Gale A, Dalton CA, Langmuir CH, Su Y, Schilling J (2013) The mean composition of ocean ridge basalts. *Geochem Geophys Geosyst* 14:489–518. 56. Lange RA, Carmichael IS (1996) The Aurora volcanic field, California-Nevada: Oxygen fugacity constraints on the development of andesitic magma. *Contrib Mineral Petrol* 125:167–185. 57. Crabtree SM, Lange RA (2012) An evaluation of the effect of degassing on the oxidation state of hydrous andesite and dacite magmas: A comparison of pre- and post-eruptive Fe²⁺ concentrations. *Contrib Mineral Petrol* 163:209–224. 58. Brounce M, Kelley K, Cottrell E (2014) Variations in Fe³⁺/ΣFe of Mariana arc basalts and mantle wedge fO₂. *J Petrol* 55:2513–2536. 59. Brounce M, Kelley KA, Cottrell E, Reagan MK (2015) Temporal evolution of mantle wedge oxygen fugacity during subduction initiation. *Geology* 43:775–778. 60. Grocke SB, Cottrell E, de Silva S, Kelley KA (2016) The role of crustal and eruptive processes versus source variations in controlling the oxidation state of iron in Central Andean magmas. *Earth Planet Sci Lett* 440:92–104. 61. Kasting JF, Egger DH, Raeburn SP (1993) Mantle redox evolution and the oxidation state of the Archean atmosphere. *J Geol* 101:245–257. 62. Kelley KA, Cottrell E (2012) The influence of magmatic differentiation on the oxidation state of Fe in a basaltic arc magma. *Earth Planet Sci Lett* 329:109–121. 63. Gentes Z (2015) Near-primary mantle melts and their implications for the mechanism of island arc basalt oxidation. Master's thesis (Univ of Rhode Island, Kingston, RI). 64. Brounce M, Stolper E, Eiler J (2017) Redox variations in Mauna Kea lavas, the oxygen fugacity of the Hawaiian plume, and the role of volcanic gases in Earth's oxygenation. *Proc Natl Acad Sci USA* 114:8997–9002. 65. Zhang HL, Cottrell E, Solheid PA, Kelley KA, Hirschmann MM (2018) Determination of Fe³⁺/ΣFe of XANES basaltic glass standards by Mössbauer spectroscopy and its application to the oxidation state of iron in MORB. *Chem Geol* 479:166–175. 66. Chinner G (1960) Pelitic gneisses with varying ferrous/ferric ratios from Glen Clova, Angus, Scotland. *J Petrol* 1:178–217. 67. Rybacki K, Kump L, Hanski E, Melezhik V (2016) Weathering during the great oxidation event: Fennoscandia, arctic Russia 2.06 Ga ago. *Precambrian Res* 275:513–525. 68. de Ronde CE, et al. (2001) Intra-oceanic subduction-related hydrothermal venting, Kermadec volcanic arc, New Zealand. *Earth Planet Sci Lett* 193:359–369. 69. Gillis KM, Robinson PT (1990) Patterns and processes of alteration in the lavas and dykes of the Troodos ophiolite, Cyprus. *J Geophys Res Solid*

Earth 95:21523–21548. 70. Bach W, Edwards KJ (2003) Iron and sulfide oxidation within the basaltic ocean crust: Implications for chemolithoautotrophic microbial biomass production. *Geochim Cosmochim Acta* 67:3871–3887. 71. Osborn EF (1959) Role of oxygen pressure in the crystallization and differentiation of basaltic magma. *Am J Sci* 257:609–647. 72. Presnall DC (1966) The join forsterite-diopside-iron oxide and its bearing on the crystallization of basaltic and ultramafic magmas. *Am J Sci* 264:753–809. 73. Juster TC, Grove TL, Perfit MR (1989) Experimental constraints on the generation of FeTi basalts, andesites, and rhyodacites at the Galapagos spreading center, 85 W and 95 W. *J Geophys Res Solid Earth* 94:9251–9274. 74. Tang M, Erdman M, Eldridge G, Lee C-TA (2018) The redox “filter” beneath magmatic orogens and the formation of continental crust. *Sci Adv* 4:eaar4444. 75. Frost BR, Lindsley DH (1992) Equilibria among Fe-Ti oxides, pyroxenes, olivine, and quartz: Part II. Application. *Am Mineral* 77:1004. 76. Snyder D, Carmichael IS, Wiebe RA (1993) Experimental study of liquid evolution in an Fe-rich, layered mafic intrusion: Constraints of Fe-Ti oxide precipitation on the TfO₂ and T-q paths of tholeiitic magmas. *Contrib Mineral Petrol* 113:73–86. 77. Toplis MJ, Carroll MR (1995) An experimental study of the influence of oxygen fugacity on Fe-Ti oxide stability, phase relations, and mineral—Melt equilibria in ferrobaltic systems. *J Petrol* 36:1137–1170. 78. Mathez EA (1984) Influence of degassing on oxidation states of basaltic magmas. *Nature* 310:371–375. 79. Candela PA (1986) The evolution of aqueous vapor from silicate melts: Effect on oxygen fugacity. *Geochim Cosmochim Acta* 50:1205–1211. 80. Carmichael IS, Ghiorso MS (1986) Oxidation-reduction relations in basic magma: A case for homogeneous equilibria. *Earth Planet Sci Lett* 78:200–210. 81. Burgisser A, Scaillet B (2007) Redox evolution of a degassing magma rising to the surface. *Nature* 445:194–197. 82. Holloway JR (2004) Redox reactions in seafloor basalts: Possible insights into silicic hydrothermal systems. *Chem Geol* 210:225–230. 83. Canil D (1997) Vanadium partitioning and the oxidation state of Archaean komatiite magmas. *Nature* 389:842–845. 84. Prytulak J, et al. (2016) Stable vanadium isotopes as a redox proxy in magmatic systems? *Geochem Perspect Lett* 3:75–84. 85. Delano JW (2001) Redox history of the Earth’s interior since approximately 3900 Ma: Implications for prebiotic molecules. *Orig Life Evol Biosph* 31:311–341. 86. Nicklas RW, Puchtel IS, Ash RD (2018) Redox state of the Archean mantle: evidence from V partitioning in 3.5–2.4 Ga komatiites. *Geochim Cosmochim Acta* 222: 447–466. 87. Turner SJ, Langmuir CH (2015) The global chemical systematics of arc front stratovolcanoes: Evaluating the role of crustal processes. *Earth Planet Sci Lett* 422:182–193. 88. Richards JP (2015) The oxidation state, and sulfur and Cu contents of arc magmas: Implications for metallogeny. *Lithos* 233:27–45. 89. Singer DA, Berger VI, Moring BC, Groat CG (2008) Porphyry copper deposits of the world: Database maps, and preliminary analysis. Open-File Report 02-268 (US Geological Survey, Reston, VA). 90. Kesler SE, Wilkinson BH (2006) The role of exhumation in the temporal distribution of ore deposits. *Econ Geol* 101:919–922. 91. Blundy J, Mavrogenes J, Tattitch B,

Sparks S, Gilmer A (2015) Generation of porphyry copper deposits by gas-brine reaction in volcanic arcs. *Nat Geosci* 8:ngeo2351. 92. Canfield DE (1994) Factors influencing organic carbon preservation in marine sediments. *Chem Geol* 114:315–329. 93. Alt JC (1995) Sulfur isotopic profile through the oceanic crust: Sulfur mobility and seawater-crustal sulfur exchange during hydrothermal alteration. *Geology* 23: 585–588. 94. Alt JC, Davidson GJ, Teagle DA, Karson JA (2003) Isotopic composition of gypsum in the Macquarie Island ophiolite: Implications for the sulfur cycle and the subsurface biosphere in oceanic crust. *Geology* 31:549–552. 95. Shanks WC, III, Bischoff JL, Rosenbauer RJ (1981) Seawater sulfate reduction and sulfur isotope fractionation in basaltic systems: Interaction of seawater with fayalite and magnetite at 200–350 C. *Geochim Cosmochim Acta* 45:1977–1995. 96. Dasgupta R (2013) Ingassing, storage, and outgassing of terrestrial carbon through geologic time. *Rev Mineral Geochem* 75:183–229. 97. Planavsky NJ, et al. (2011) Widespread iron-rich conditions in the mid-Proterozoic ocean. *Nature* 477:448–451. 98. Bachan A, Kump LR (2015) The rise of oxygen and siderite oxidation during the Lomagundi event. *Proc Natl Acad Sci USA* 112:6562–6567. 99. Blättler CL, et al. (2018) Two-billion-year-old evaporites capture Earth’s great oxidation. *Science* 360:320–323. 100. Canfield DE (1998) A new model for Proterozoic ocean chemistry. *Nature* 396: 450–453. 101. Walker D, Shibata T, DeLong SE (1979) Abyssal tholeiites from the Oceanographer fracture zone. *Contrib Mineral Petrol* 70:111–125. 102. Zimmer MM, et al. (2010) The role of water in generating the calc-alkaline trend: New volatile data for Aleutian magmas and a new tholeiitic index. *J Petrol* 51: 2411–2444. 103. Miyashiro A (1974) Volcanic rock series in island arcs and active continental margins. *Am J Sci* 274:321–355. 104. Brown GC (1981) Space and time in granite plutonism. *Philos Trans R Soc Lond Ser Math Phys Sci* 301:321–336. 105. Laurent O, Martin H, Moyen J-F, Doucelance R (2014) The diversity and evolution of late-Archean granitoids: Evidence for the onset of “modern-style” plate tectonics between 3.0 and 2.5 Ga. *Lithos* 205:208–235. 106. Sisson TW, Grove TL (1993) Experimental investigations of the role of H₂O in calcalkaline differentiation and subduction zone magmatism. *Contrib Mineral Petrol* 113:143–166. 107. Grove TL, Brown SM (2018) Magmatic processes leading to compositional diversity in igneous rocks: Bowen (1928) revisited. *Am J Sci* 318:1–28. 108. Kump LR, Kasting JF, Barley ME (2001) Rise of atmospheric oxygen and the “upsidedown” Archean mantle. *Geochim Geophys Geosyst* 2:1525–2027. 109. Holland HD (2002) Volcanic gases, black smokers, and the great oxidation event. *Geochim Cosmochim Acta* 66:3811–3826.